Role of the D Arm and the Anticodon Arm in tRNA Recognition by Eubacterial and Eukaryotic RNase P Enzymes†

Wolf-Dietrich Hardt, Judith Schlegl, Volker A. Erdmann, and Roland K. Hartmann*

Institut für Biochemie, Freie Universität Berlin, Thielallee 63, 14195 Berlin, FRG

Received April 9, 1993; Revised Manuscript Received September 1, 1993®

ABSTRACT: Truncated precursor tRNAs lacking the D arm or anticodon arm were studied *in vitro* as substrates for RNase P enzymes from *Escherichia coli*, *Thermus thermophilus* (eubacteria), and HeLa. Deletion of the D arm still allowed 5′-processing by *E. coli* RNase P, but strongly impaired maturation by *T. thermophilus* and HeLa extracts. In contrast, deletion of the anticodon arm had no influence on processing by RNase P activities from all three organisms. Inhibition kinetics and gel retardation studies showed that deletion of the D arm leads to low-affinity binding to *E. coli* RNase P RNA (M1 RNA). However, the *E. coli* enzyme appears to form sufficiently strong contacts in the region of the T arm, acceptor stem, and CCA terminus to still allow productive enzyme–substrate interaction even in the absence of the structural contribution provided by the D arm. Pb^{2+}-induced hydrolysis of a $tRNA^{Gly}$ from *T. thermophilus* gave identical cleavage patterns in the D arm and anticodon loop in the absence and presence of *E. coli* M1 RNA, whereas lead hydrolysis was strongly reduced at the CU*CCA*A 3′-terminus due to the presence of the enzyme.

Ribonuclease P (RNase P)[1] is a ubiquitous ribonucleoprotein particle that cleaves tRNA precursors and so generates their mature 5′-termini. In eubacteria, it is composed of a large RNA subunit, approximately 400 nt in size, and a small basic protein of approximately 120 amino acids (Brown & Pace, 1992). RNA subunits of eubacterial RNase P enzymes were shown to be catalytically active in the absence of protein components (Guerrier-Takada et al., 1983). Catalysis by isolated RNA subunits of RNase P from eukaryotic nuclei, mitochondria, or archaebacteria has not been demonstrated so far.

The acceptor stem and the T arm have been identified as essential structural elements for substrate recognition by RNase P in chemical modification interference studies (Kahle et al., 1990; Thurlow et al., 1991; Gaur & Krupp, 1993). Truncated tRNAs consisting of the acceptor stem, CCA terminus, and T arm, and even an acceptor microhelix with a CCA end, can be processed by *Escherichia coli* RNase P (McClain et al., 1987; Forster & Altman, 1990). Such substrates were cleaved at very low rates by RNase P and RNase P RNA from *Thermus thermophilus*, an extreme thermophilic eubacterium, indicating that minimal structural requirements for efficient processing of substrates differ even among related eubacterial RNase P enzymes (Schlegl et al., 1992). These observations prompted us to analyze tRNA derivatives that include additional structural elements beyond the acceptor stem and the T arm.

Naturally occurring tRNAs with deletions of the dihydrouridine arm (D-replacement tRNAs) have been identified in mitochondria of mammals, *Drosophila*, nematodes, and trematodes (De Bruijn & Klug, 1983, 1984; Garey & Wolstenholme, 1989; Okimoto & Wolstenholme, 1990). Tertiary structures, similar to the L shape of normal tRNAs, were proposed for D-replacement tRNAs (De Bruijn & Klug, 1983, 1984). These molecules may be stabilized by tertiary interactions between single-stranded D-replacement nucleotides and T-loop bases, as well as by extensions of the anticodon stem by two base pairs (De Bruijn & Klug, 1983, 1984). This may, at least partly, compensate for the major disruptions of the tertiary structure expected to result from deletion of the D arm (Quigley & Rich, 1976). A D-replacement derivative of an amber suppressor $tRNA^{Phe}$ from *E. coli*, including the D-replacement loop and the enlarged T loop of bovine mitochondrial $tRNA^{Ser}$, was shown to be cleaved by *E. coli* RNase P (McClain et al., 1987). To further evaluate the role of the D arm for processing by RNase P enzymes, we analyzed the following substrates in reactions catalyzed by *E. coli* and *T. thermophilus* RNase P and by HeLa RNase P: two serine-specific tRNAs from human and bovine mitochondria and four derivatives (DR1–4) of a class I $tRNA^{Gly}$ from *T. thermophilus* (Hartmann et al., 1991). We also analyzed variants of the *T. thermophilus* $tRNA^{Gly}$, which carried deletions of the anticodon arm (Figure 1).

The structures of $tRNA^{Gly}$ and one tRNA variant lacking the D arm were probed by Pb^{2+}-induced hydrolysis in the presence or absence of *E. coli* M1 RNA.

MATERIALS AND METHODS

PCR Amplification. The *T. thermophilus* $tRNA^{Gly}$ gene (Hartmann et al., 1991) or DNA oligonucleotides were used as templates for PCR amplification as described (Schlegl et al., 1992). PCR primers for the 3′ region were 20 nucleotides in length, and primers for the 5′ region contained 17 nucleotides of T7 promoter sequences (Milligan & Uhlenbeck, 1989)

† Supported by the Deutsche Forschungsgemeinschaft (SFB 9/B5, SFB 344/C2/D6, and Gottfried Wilhelm Leibniz-Programm) and the Fonds der Chemischen Industrie e.V. W.-D.H receives a stipend from the Boehringer Ingelheim Fonds.

* Address correspondence to this author. Telephone: 30-838 6023. Fax: 30-838 6403.

® Abstract published in *Advance ACS Abstracts,* November 1, 1993.

[1] Abbreviations: RNase P, ribonuclease P; DTE, 1,4-dithioerythritol; SDS, sodium dodecyl sulfate; PMSF, phenylmethanesulfonyl fluoride; PEG, poly(ethylene glycol); EDTA, ethylenediaminetetraacetic acid; Tris, tris(hydroxymethyl)aminomethane; PCR, polymerase chain reaction; DEPC, diethyl pyrocarbonate; k_{cat}, moles of substrate cleaved per minute and mole of enzyme at saturating substrate concentrations; $k_{observed}$, moles of substrate cleaved per minute and mole of enzyme at 0.4 μM substrate; appK_d, apparent equilibrium dissociation constant (see Materials and Methods).

0006-2960/93/0432-13046$04.00/0

followed by 20 nucleotides complementary to the PCR template DNA. DNA amplification assays were performed with *Taq* or *Pfu* DNA polymerase as recommended by the manufacturer (Stratagene).

Preparation of RNAs. *E. coli* and *T. thermophilus* RNase P RNAs were transcribed from the T7 expression plasmids pJA2 (Vioque et al., 1988), linearized with *Fok*I, and pT7M1HB8 (Hartmann & Erdmann, 1991), linearized with *Nar*I. Pre-4.5S RNA was transcribed from the plasmid T7-4.5S (a gift from R. A. Lempicki and M. J. Fournier). Substrate RNAs (Figure 1) were synthesized as runoff transcripts with T7 RNA polymerase using PCR-amplified templates carrying the T7 promoter sequence, [α-^{32}P]CTP (25 μCi) was included for the preparation of radioactive transcripts. Mature tRNA^{Gly} starting with a 5′-monophosphate was synthesized by T7 transcription including 5′-GMP as described (Milligan & Uhlenbeck, 1989). Products were purified by electrophoresis in polyacrylamide gels containing 8 M urea and were recovered from gels as described recently (Schlegl et al., 1992). *E. coli* M1 RNA was 3′-end-labeled with [5′-^{32}P]pCp using T4 RNA ligase (England & Uhlenbeck, 1978).

Partial purification of holoenzyme activities from *E. coli* and *T. thermophilus* was performed as described (Schlegl et al., 1992). HeLa extracts were prepared as previously reported (Dignam et al., 1983).

Processing Assays. Cleavage assays using RNase P RNAs from *E. coli* and *T. thermophilus* were performed in M1-mix [50 mM glycine/NaOH, pH 7.5, 100 mM $MgCl_2$, 100 mM NH_4Cl, 4% PEG 6000 (Merck), and 0.5% (w/v) SDS] or 1 × TAMN (see below); buffer conditions for processing by RNase P holoenzymes from the two eubacteria have been described recently (Schlegl et al., 1992). Assays with HeLa extracts were performed in 30 mM Tris-HCl, pH 7.5, 5 mM $MgCl_2$, 200 mM NH_4Cl, and 0.5 mM DTE at 37 °C. Enzymes and substrates were preincubated separately for 10 min under respective reaction conditions. Reactions were started by mixing prewarmed enzyme and substrate mixtures, and aliquots were withdrawn at different times. For reactions catalyzed by RNase P RNAs, initial velocities were expressed as $k_{observed}$ (k_{obs}) values, which correspond to moles of substrate converted per mole of enzyme per minute at 0.4 μM substrate and 0.1 μM enzyme, if not stated otherwise. Values of K_m and k_{cat} ($v_{max}/[E]_{total}$) for multiple turnover reactions were determined by Lineweaver–Burk plots.

Gel Retardation Assays. ^{32}P-Labeled substrate or product RNAs and *E. coli* RNase P RNA (M1 RNA) were preincubated in 50 mM Tris–acetate, pH 7.0, 5% glycerol, 100 mM NH_4OAc, and 100 mM $Mg(OAc)_2$ at 37 °C for 7–10 min in a total volume of 10 μL, if not stated otherwise. Samples were loaded (under current) on 5% polyacrylamide gels prewarmed at 37 °C and equilibrated in 1 × TAMN buffer [50 mM Tris–acetate, 100 mM $Mg(OAc)_2$, 100 mM NH_4OAc, and 2 mM EDTA, pH 7.0]. Electrophoresis conditions were adjusted to obtain a gel temperature of 37 °C, and separation was accomplished after 10–20 h. Gels were dried on Whatman 3MM paper before autoradiography; bands were excised, and the radioactivity was determined by Cerenkov counting. Equilibrium binding was measured by M1 RNA concentration variation experiments at a constant tRNA concentration of 0.1 μM. The equilibrium dissociation constant K_d for the tRNA–M1 RNA complex can be calculated according to the following equation (Pyle et al., 1990): $K_d = [\text{M1 RNA}]_{\text{total at 50\% complex}} - 0.5[P]_{total}$ where P corresponds to the tRNA. Since binding curves display nonhyperbolic M1 RNA concentration dependences [for a detailed discussion, see Hardt et al. (1993)], we have measured complex formation at the constant tRNA concentration of 0.1 μM, and K_d values are given as apparent K_d values (appK_d). M1 RNA concentrations measured by UV absorption were corrected by a factor of 0.55, since only 50–60% of the M1 RNA molecules were found to rapidly bind a tRNA molecule (Hardt et al., 1993). The free binding energies were calculated as $\Delta G° = -RT \ln(1/K_d)$, with R = 0.00198 kcal mol^{-1} K^{-1} and T in kelvin (Pyle et al., 1990).

Hydrolysis by Pb^{2+} Ions. Lead cleavage was performed essentially as described previously (Ciesiolka et al., 1992a,b). In detail, 3′-^{32}P-labeled RNAs (25 ng) were preincubated for 10 min at 37 °C in 125 mM $Mg(OAc)_2$, 125 mM NH_4OAc, and 62.5 mM Tris-HCl, pH 7.1. The amount of RNA was adjusted to 1.5 μg/4-μL sample either with *E. coli* pre-4.5 S RNA (as a control) or with M1 RNA. The cleavage reaction was started by the addition of 1 μL of lead acetate solution to yield final Pb^{2+} concentrations of 100, 50, or 20 mM. In control lanes, 1 μL of water was added. After a 15-min incubation at 37 °C, cleavage was stopped by addition of 7 μL of loading buffer (67% formamide, 0.3 × TBE, 2.7 M urea, and 100 mM EDTA) and shock-freezing in liquid nitrogen. Hydrolysis products were separated on 10% or 25% polyacrylamide–8 M urea gels and visualized by autoradiography.

RESULTS

Structure of Substrates. The glycine-specific pre-tRNA from *T. thermophilus* (Hartmann et al., 1991) was used as the reference molecule in this study (Figure 1). This tRNA was expected to have a rigid structure due to its high G/C content in stem regions. The primary sequence includes all the generally conserved positions (Sprinzl et al., 1989). A second class I, but eukaryotic-type pre-tRNA^{Gly} from *Homo sapiens sapiens* was used as a second reference substrate, which closely resembles the consensus structure for mammalian tRNAs according to Sprinzl et al. (1989). One idiosyncrasy of the human tRNA^{Gly} is a D stem expected to be rather weak due to two A-U base pairs and one terminal G-U pair (Figure 1). The human tRNA^{Gly}, as well as all other tested substrates, was synthesized with the natural 5′ flank (14 nt) of the *T. thermophilus* pre-tRNA^{Gly} (Hartmann et al., 1991; Figure 1). This ensured that observed differences in cleavage efficiencies of the two tRNAs were attributable to mature domains.

Our study included naturally occurring mitochondrial (mt) serine-tRNAs lacking the D arm (Figure 1). The structure of tRNA^{Ser} from bovine mitochondria has been investigated in detail (De Bruijn & Klug, 1983, 1984). Peculiarities of the two mt serine-tRNAs are A-U-rich acceptor stems, irregular and extended anticodon stems, and deviations in size and sequence from the conserved T-loop structure. The bovine and human mt serine-tRNAs display significant differences to each other in primary sequence and secondary structure (De Bruijn & Klug, 1984; Figure 1).

Proceeding from the mt serine-tRNA structures, we designed a set of derivatives of the pre-tRNA^{Gly} from *T. thermophilus* which lack the D arm (Figure 1). Variants DR1–4 display minor differences in the central core of the tRNA structure, which may result in different relative orientations of the two arms of the L-shaped tertiary structure. The acceptor stem and T arm remained unchanged. In detail, deletions involved nucleotides 10–24 (DR3), 10–25 (DR1),

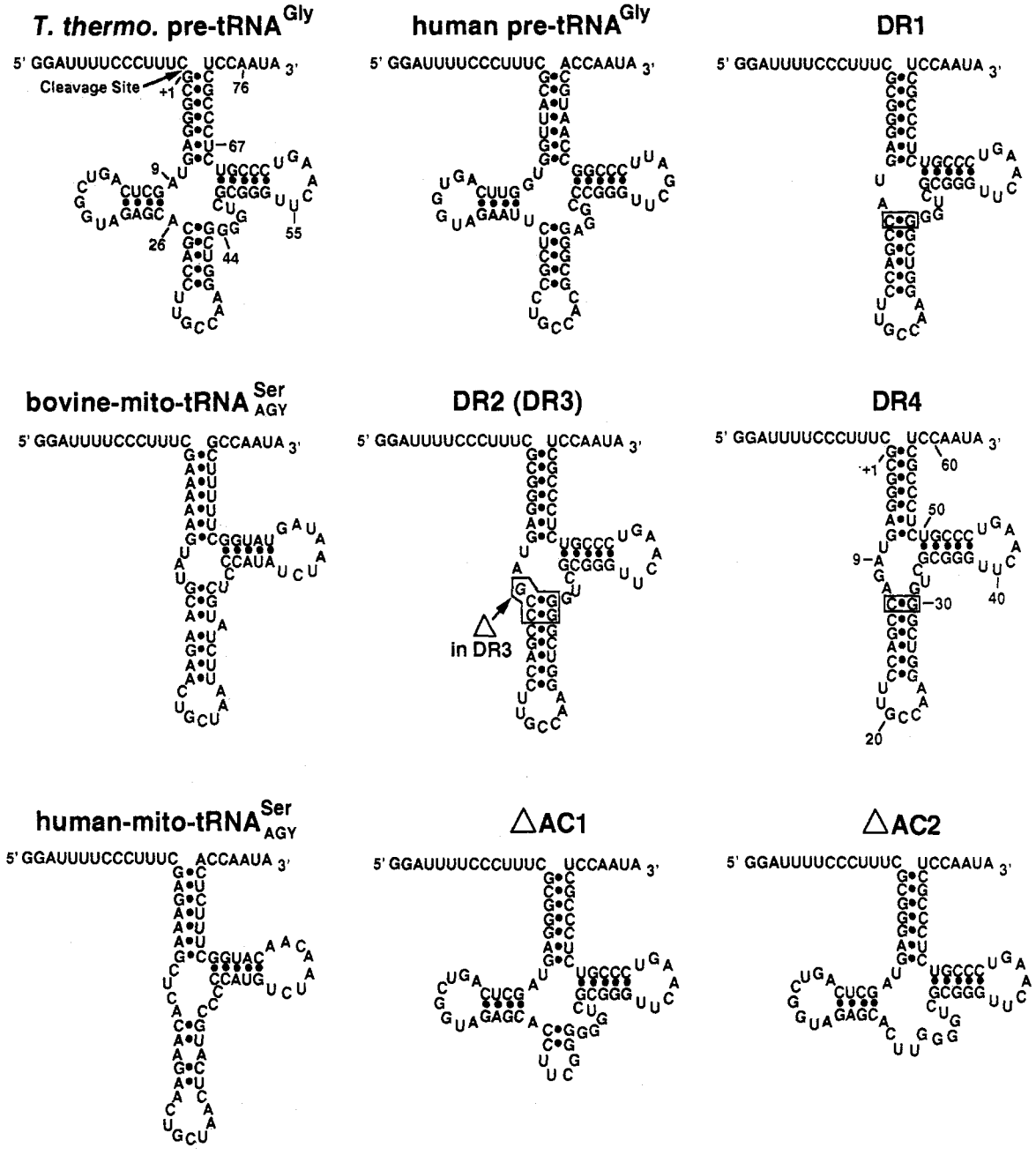

FIGURE 1: Secondary structures of model substrates for RNase P RNA subunits and holoenzymes. The *T. thermophilus* pre-tRNA^{Gly}, encoded in the two 23S–5S rRNA operons of *T. thermophilus*, carries its naturally occurring 5′- and 3′-flanking sequences (Hartmann et al., 1991). All other substrates shown were endowed with these flanking sequences. Sequences of the human pre-tRNA^{Gly} and the mammalian mitochondrial tRNAs were taken from Sprinzl et al. (1989).

11–24 (DR2), and 11–25 (DR4) of tRNA^{Gly}. A26 was replaced by C in DR1–3, and DR4 carried an inserted C subsequent to A26 as well as a deletion of G44 (Figure 1). These nucleotide changes were introduced to extend the anticodon stem by one or two base pairs, which may stabilize the structure of the core region.

To assess the role of the anticodon arm in 5′-maturation catalyzed by RNase P enzymes, we analyzed two additional variants of the *T. thermophilus* precursor-tRNA^{Gly} (Figure 1). In variant ΔAC1, a short microhelix replacing the anticodon arm may form, whereas in RNA ΔAC2 the anticodon arm was replaced by a CUUG tetraloop sequence (Figure 1).

Processing by T. thermophilus RNase P RNA and Holoenzyme. The human pre-tRNA^{Gly} was processed by the thermophilic enzyme, although less efficiently than the bacterial pre-tRNA^{Gly} (Table I), while tRNAs with D-arm deletions were poor substrates for RNase P RNA and the holoenzyme of *T. thermophilus* (Table I). Cleavage by this RNase P RNA was reduced 50-fold or more, with DR4 being the best substrate among them. Cleavage efficiencies of mammalian mt tRNAs by *T. thermophilus* RNase P RNA or holoenzyme were even further decreased. In contrast, RNAs ΔAC1 and ΔAC2 were processed with high efficiency (Table I). A slightly better kinetic performance of ΔAC1 may be assigned to the stabilizing microhelix which is missing in ΔAC2 (Figure 1).

Processing in HeLa Extracts. Substrate preferences similar to those of the *T. thermophilus* enzyme were observed with the eukaryotic extract (Table I). Accordingly, precursor tRNAs lacking the D arm were rather poor substrates, whereas those lacking the anticodon arm were processed efficaciously.

Table I: Relative Cleavage Efficiencies of Model Substrates for RNase P RNAs and Holoenzymes[a]

substrate	A (k_{obs}, min^{-1}) for RNase P RNA		B (relative activity, %) for RNase P		
	E. coli	*T. thermophilus*	*E. coli*	*T. thermophilus*	HeLa
T. thermophilus $ptRNA^{Gly}$	0.2	1.0	100	100	100
human $ptRNA^{Gly}$	0.2	0.1	30	30	50
DR1	0.04	<0.02	40	4	<3
DR2	0.04	<0.02	30	1	3
DR3	0.035	<0.02	40	2	<3
DR4	0.13	0.02	40	5	3
human mito $ptRNA^{Ser}$	0.005	<0.01	20	<1	1
bovine mito $ptRNA^{Ser}$	0.001	<0.01	20	<1	3
ΔAC1	0.09	1.5	140	88	71
ΔAC2	0.11	0.6	100	65	71

[a] Column A: Kinetics were performed in M1-mix using 0.1 μM RNase P RNA and 0.4 μM substrate RNAs, except for cleavage of pre-$tRNA^{Gly}$ ($ptRNA^{Gly}$) by *T. thermophilus* RNase P RNA (10 nM). Cleavage rates were deduced from the linear range of curves; k_{obs} is given in moles of product formed per mole of enzyme per minute at the substrate concentrations indicated above. Column B: Relative cleavage efficiencies of substrates for RNase P holoenzymes from *E. coli*, *T. thermophilus*, and HeLa extracts were deduced from linear ranges of curves. Values were normalized to cleavage of pre-$tRNA^{Gly}$ (=100%), and values of 100% in reactions catalyzed by the different RNase P enzymes are not interrelated since specific activities were not determined.

Table II: Kinetic and Equilibrium Dissociation Constants for Cleavage by *E. coli* M1 RNA[a]

	M1-mix		1 × TAMN	
	k_{cat} (min^{-1})	K_m (μM)	k_{cat} (min^{-1})	appK_d (μM)
pre-$tRNA^{Gly}$	0.4	0.2	0.5	0.07
DR4	0.4	1.5	0.8	1.6
ΔAC1	0.4	0.05	0.4	0.1
ΔAC2	0.3	nd	0.3	0.1

[a] Constants were determined in two different buffer systems (M1-mix and 1 × TAMN; see Materials and Methods); appK_d values for the mature RNAs were determined by gel retardation analysis (Figures 3 and 4, Materials and Methods); K_m and k_{cat} were measured for the multiple turnover reaction and derived from Lineweaver–Burk plots.

Table III: Cleavage of Substrates between Nucleotides −2 and −1 as Percent of Total Cleavage[a]

substrate	% cleavage between nt −2 and −1			
	E. coli		*T. thermophilus*	
	RNA	holoenzyme	RNA	holoenzyme
$ptRNA^{Gly}$ *T. thermophilus*	3	3	2	3
$ptRNA^{Gly}$ human	21	19	15	20
DR1	26	19	nd	nd
DR2	16	15	nd	nd
DR3	15	13	nd	nd
DR4	20	20	nd	16

[a] nd, not determined due to low cleavage efficiencies.

It is unclear whether these substrate preferences are solely attributable to nuclear RNase P since the procedure employed for the preparation of HeLa nuclear extracts (Dignam et al., 1983) does not exclude contaminations by mitochondrial processing enzymes.

Processing by E. coli M1 RNA and RNase P. Deletion of the D arm caused no dramatic loss of cleavage activity in reactions catalyzed by *E. coli* M1 RNA and RNase P (Table I). For the reaction catalyzed by M1 RNA, substrates could be subdivided into three groups of slightly different kinetic performance: precursors of the bacterial and human $tRNA^{Gly}$, ΔAC1 and ΔAC2, as well as DR4 belonged to the group of highest turnover (k_{obs} = 0.1–0.2 min^{-1}). DR1, DR2, and DR3 showed medium rates with k_{obs} values around 0.04 min^{-1} while the mammalian mt pre-tRNAs were cleaved less efficiently (Table I). A hairpin substrate mimicking the coaxially stacked acceptor stem and T arm of the *T. thermophilus* $tRNA^{Gly}$ yielded cleavage rates similar to DR1–3 under identical assay conditions (k_{obs} = 0.012 min^{-1}; Schlegl et al., 1992). Differences in efficiency were less pronounced in the reaction catalyzed by the holoenzyme. Even cleavage rates for the two mitochondrial tRNAs reached 20% of that obtained for the pre-$tRNA^{Gly}$. The two RNAs carrying deletions of the anticodon arm were processed as efficaciously as the bacterial pre-$tRNA^{Gly}$ (Table I). K_m and k_{cat} values have been determined for DR4, pre-$tRNA^{Gly}$, and ΔAC1 under conditions of multiple turnover in the reaction catalyzed by M1 RNA (Table II). Values were very similar for pre-$tRNA^{Gly}$ and ΔAC1, whereas the K_m for DR4 was significantly higher.

Determination of Processing Sites. Processing sites were analyzed for precursors of the two glycine-tRNAs and DR1–4 in reactions catalyzed by the two bacterial RNase P enzymes and their catalytic RNA subunits. The predominant cleavage site was located between C −1 and G +1 (arrow in Figure 1) in all cases. Additionally, aberrant cleavage between U −2 and C −1 was quantified by band excision and Cerenkov counting in those cases where cleavage efficiencies were sufficiently high (Table III). All substrates showed 15–20% secondary cleavage between U −2 and C −1, with the exception of *T. thermophilus* pre-$tRNA^{Gly}$ giving rise to only 3%. No cleavage was seen in controls in the absence of enzyme. In addition, the ratio of cleavage at the two positions was constant at different time points of substrate conversion. Thus, we could exclude that the liberated 5′-flank (14 nucleotides) might have been shortened in a subsequent step to yield the 13-nt flank attributed to aberrant cleavage. These results, which were independent of the enzymatic activity or the reaction temperature (37 °C for *E. coli* and 55 °C for *T. thermophilus* RNase P RNAs and holoenzymes), suggest that cleavage site selection is inherently determined by the substrate RNAs investigated here.

Inhibition Experiments. DR4 was analyzed as an inhibitor of pre-$tRNA^{Gly}$ cleavage in the reaction catalyzed by *E. coli* M1 RNA. For this purpose, conversion of 0.4 μM ^{32}P-labeled pre-$tRNA^{Gly}$ to mature tRNA was measured in the presence of 2 μM either unprocessed DR4 (DR4), mature DR4 (mDR4), pre-$tRNA^{Gly}$ ($ptRNA^{Gly}$), or mature $tRNA^{Gly}$ (Figure 2A). The weak inhibition of ^{32}P-labeled pre-$tRNA^{Gly}$ processing by DR4 and mDR4 indicates a low affinity of this RNA to *E. coli* M1 RNA. This is consistent with higher K_m and appK_d values measured for this variant (Table II).

In addition, precursor substrates displayed the same inhibitory effect as their mature products (Figure 2A). Identical results were obtained with pre-$tRNA^{Gly}$ completely processed during preincubation (Figure 2A, ■) and T7 transcripts of mature $tRNA^{Gly}$ (Figure 2B, ♦). Of course, it has to be considered that inhibitor substrates were also converted to product during the course of the reaction. However, essentially identical initial rates of ^{32}P-labeled pre-$tRNA^{Gly}$ conversion in the presence of unlabeled precursor or mature tRNA and DR4 indicate that the 14-nt 5′-flank had no influence on binding to *E. coli* M1 RNA. In accordance, mature tRNA has been shown to be a purely competitive inhibitor in the pre-tRNA cleavage reaction of RNase P RNA (Smith et al., 1992), indicating that precursor and mature tRNAs occupy the same site. For cleavage of pre-$tRNA^{Tyr}$

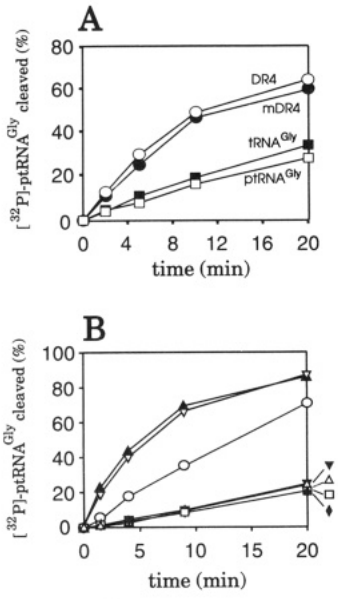

FIGURE 2: Inhibition of ^{32}P-labeled *T. thermophilus* pre-tRNA^{Gly} cleavage by excess amounts of unlabeled inhibitor RNAs. (A) Inhibition by pre-tRNA^{Gly} (ptRNA^{Gly}, □), tRNA^{Gly} (■), unprocessed DR4 (DR4, ○), and mature DR4 (mDR4, ●). Assays were performed as follows: for inhibition by products, 4.2 pmol of *E. coli* M1 RNA was preincubated with 84 pmol of unlabeled pre-tRNA^{Gly} or DR4 for 2 h at 37 °C in 21 μL of M1-mix, which led to complete substrate conversion as confirmed by control experiments (data not shown); reactions were started by the addition of 21 μL of M1-mix containing 16.8 pmol of ^{32}P-labeled pre-tRNA^{Gly} which had been preincubated separately for 2 h at 37 °C; final concentrations were 0.1 μM *E. coli* M1 RNA, 0.4 μM ^{32}P-labeled pre-tRNA^{Gly}, and 2 μM unlabeled inhibitor RNA. For inhibition by substrates, 16.8 pmol of ^{32}P-labeled pre-tRNA^{Gly} was preincubated with 84 pmol of pre-tRNA^{Gly} or DR4 for 2 h at 37 °C in 21 μL of M1-mix; reactions were started by addition of 21 μL of M1-mix containing 4.2 pmol of M1 RNA which had been preincubated separately for 2 h at 37 °C. The reaction was followed by maturation of ^{32}P-labeled pre-tRNA^{Gly} (in %) without correcting for the total concentration of substrate. (**B**) Inhibition of ^{32}P-labeled pre-tRNA^{Gly} cleavage by excess amounts of unlabeled pre-tRNA^{Gly} (□), tRNA^{Gly} (♦, mature T7 transcript with 5′-monophosphate; see Materials and Methods), and precursor RNAs DR2 (▲), DR4 (○), ΔAC1 (△), and ΔAC2 (▼); (▽) no inhibitor RNA added. Assays were performed with final concentrations of 0.1 μM *E. coli* M1 RNA, 0.4 μM ^{32}P-labeled pre-tRNA^{Gly}, and 2 μM unlabeled inhibitor RNA; the latter two RNAs were preincubated for 10 min at 37 °C in M1-mix; reactions were started by adding M1 RNA which had been preincubated separately for 10 min at 37 °C in the same buffer.

by *E. coli* M1 RNA, the product of the reaction has been tested as inhibitor (Tallsjö & Kirsebom, 1993). K_i was very similar to K_m, suggesting that the product of the reaction interacts with M1 RNA as efficiently as the substrate. Likewise, we could not observe any difference in processing of ^{32}P-labeled pre-tRNA^{Gly} (0.4 μM, 0.1 μM *E. coli* M1 RNA) in the absence or presence of exogenously added 2 μM 5′-flank (14 nt, chemically synthesized; data not shown). We like to note that, in contrast to this 5′-flank, other 5′-flanking sequences may be involved in binding to M1 RNA (Guerrier-Takada & Altman, 1993).

No inhibition was observed in the case of DR2 (Figure 2B, ▲), since the cleavage rate was identical to that of ^{32}P-labeled pre-tRNA^{Gly} when no inhibitor RNA was present. RNAs ΔAC1 (△) and ΔAC2 (▼) had the same inhibitory effect as tRNA^{Gly} (♦, Figure 2B). In this context, DR4 (○) was an inhibitor of intermediate strength. Though the simple inhibition experiments (Figure 2) are not conclusive by themselves, they are in good correlation with the results obtained by gel retardation; i.e., strong inhibitors show low equilibrium binding

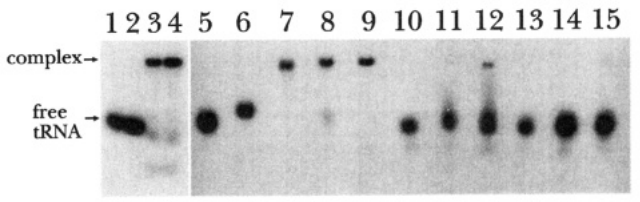

FIGURE 3: Equilibrium binding of tRNAs and tRNA derivatives to *E. coli* M1 RNA. In lanes 3, 4, and 8–15, ^{32}P-labeled substrate RNAs (0.1 μM) were incubated for 10 min with a 5 molar excess of M1 RNA in 1 × TAMN and were loaded on the 5% polyacrylamide gel equilibrated with the same buffer. Lanes: 3, mΔAC2; 4, mΔACl; 8, human tRNA^{Gly}; 9, *T. thermophilus* tRNA^{Gly}; 10, bovine mt tRNA^{Ser}; 11, human mt tRNA^{Ser}; 12, mDR4,; 13, mDR1; 14, mDR3; 15, mDR2. Control lanes: 7,3′-^{32}P-labeled *E. coli* M1 RNA; lanes 1, 2, 5, and 6, ΔAC2 (1), ΔAC1 (2), DR4 (5), and *T. thermophilus* pre-tRNA^{Gly} (6) in the absence of M1 RNA.

constants. Likewise, variants of *T. thermophilus* tRNA^{Gly} lacking nucleotide +1 or 3′-nucleotides were weak inhibitors and bound with low affinity to M1 RNA (Hardt et al., 1993; unpublished results).

Gel Retardation Assays. We haved used a gel retardation assay to measure the affinities of truncated tRNA substrates to *E. coli* M1 RNA under processing assay conditions (Figure 3). Cleavage rates were practically identical in M1-mix and 1 × TAMN buffers used for the gel shift assay (Table II). Under conditions used for gel retardation assays, all substrates, except for the two mitochondrial pre-tRNAs, were cleaved to more than 90% prior to gel application (data not shown). Thus, we measure equilibrium binding of product to the enzyme (except for the mt pre-tRNAs). However, identical results were attained with pre-tRNA^{Gly} and mature tRNA^{Gly}, and exogenously added 14-nt 5′-flank had no influence on complex formation (data not shown).

Almost 100% of the *T. thermophilus* tRNA^{Gly} and 80% of the human tRNA^{Gly} were shifted into a complex (Figure 3, lanes 8 and 9) which roughly comigrated with ^{32}P-labeled M1 RNA (lane 7). Recent data show that this complex can be separated physically from M1 RNA alone in an optimized gel system (Hardt et al., 1993). No complex formation was observed with DR1–3 (lanes 13–15) and mammalian mt tRNAs (lanes 10 and 11) under these conditions. However, 14% of mature DR4 (mDR4) was shifted into the complex with M1 RNA (lane 12). Thus, among the D-replacement tRNAs analyzed (Figure 1), DR4 not only showed the highest cleavage efficiency (Table I) but also bound (in its mature form) with the highest affinity to *E. coli* M1 RNA under equilibrium conditions, and was the most efficient inhibitor of cleavage among D-replacement tRNAs (Figure 2). RNAs mΔAC1 and mΔAC2, as the intact tRNA^{Gly}, were almost completely shifted into the complex (Figure 3, lanes 3 and 4). Control lanes in the absence of *E. coli* M1 RNA (Figure 3, lanes 1, 2, 5, and 6) show that the observed complexes are not due to tRNA aggregates.

To determine the apparent equilibrium dissociation constant appK_d for *E. coli* M1 RNA–tRNA complexes, substrates (0.1 μM) were incubated with increasing amounts of M1 RNA and analyzed by native polyacrylamide gel electrophoresis (Figure 4). On the basis of these results, appK_d values of 0.07 μM for tRNA^{Gly}, 0.1 μM for mΔAC1 and mΔAC2, and 1.6 μM for mDR4 were calculated (Table II, see Materials and Methods). An appK_d values of 0.1 μM corresponds to a binding free energy of approximately −10 kcal/mol at 37 °C, compared to −8.2 kcal/mol for equilibrium binding of mDR4 to *E. coli* M1 RNA (see Materials and Methods). This difference would be equivalent to the loss of one hydrogen bond in complexes of mDR4 and M1 RNA.

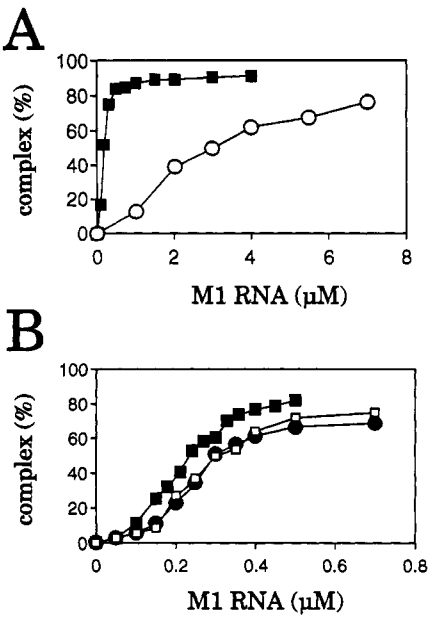

FIGURE 4: Equilibrium binding of *T. thermophilus* $tRNA^{Gly}$, mDR4, mature ΔAC1 (mΔAC1), and mature ΔAC2 (mΔAC2) to *E. coli* M1 RNA. Constant amounts of ^{32}P-labeled substrate RNAs (0.1 μM) were incubated for 5 min at 37 °C with increasing amounts of M1 RNA in 1 × TAMN and loaded on the 5% polyacylamide gel equilibrated with the same buffer. Binding curves were deduced from gel retardation assays similar to those shown in Figure 3; radioactive bands were visualized by autoradiography, excised from the gel and Cerenkov-counted. (A) Binding curves for $tRNA^{Gly}$ (■) and mDR4 (○); (B) binding curves for $tRNA^{Gly}$ (■), mΔAC1 (□), and mΔAC2 (●).

Pb^{2+}-Induced Hydrolysis of DR4 and $tRNA^{Gly}$. Pb^{2+}-induced hydrolysis of RNA can occur at specific sites due to the presence of tight metal ion binding sites. For example, yeast $tRNA^{Phe}$ is cleaved specifically between nucleotides 17 and 18 in the D loop (Brown et al., 1985; Krzyosiak et al., 1988; Behlen et al., 1990). Cleavages of lower intensity are observed at higher Pb^{2+} concentrations with a marked preference for single-stranded regions of RNAs (Krzyzosiak et al., 1988; Ciesiolka et al., 1992 a,b).

The predominant site of Pb^{2+} hydrolysis in the D loop of *T. thermophilus* $tRNA^{Gly}$ was located between G15 and U16, and weaker cleavage sites were found between nt 16 and 18, as well as between nt 19 and 21; further sites of cleavage were in the anticodon loop (nt 33–37) and at the 3′-end (Figure 5; nt 72–76; see Figure 1). DR4 showed a cleavage pattern consistent with the secondary structure as drawn in Figure 1.

Lead cleavage patterns at 10 mM Mg^{2+} and 0.5–5 mM Pb^{2+} (data not shown) were identical to those at 100 mM Mg^{2+} and up to 100 mM Pb^{2+} (Figure 5), suggesting that elevated Mg^{2+} and Pb^{2+} concentrations had no significant effect on tRNA structure. In addition, pre-$tRNA^{Gly}$ and mature $tRNA^{Gly}$ showed no differences in susceptibility to Pb^{2+}-induced hydrolysis (data not shown).

We then compared Pb^{2+} cleavage for $tRNA^{Gly}$ and DR4 in the presence of excess amounts of either precursor 4.5 S RNA (as controls) or M1 RNA from *E. coli* (Figure 5). Inferred from gel retardation experiments under similar conditions, all $tRNA^{Gly}$ and DR4 is expected to be trapped in the complex with M1 RNA. In the presence of *E. coli* M1 RNA, strong protection from Pb^{2+} hydrolysis was observed at the CCA terminus of both DR4 and $tRNA^{Gly}$ (corresponding to nt 72–77 of $tRNA^{Gly}$, Figure 1). Further regions of protection in DR4 were in the T loop (nt 39–43 of DR4, Figure 1) and T stem, particularly at the first G-U base pair of the T stem. Corresponding results could not be attained with $tRNA^{Gly}$ due to its low susceptibility to lead-induced hydrolysis in the T arm even in the absence of M1 RNA. The susceptibilities of D-loop nucleotides in $tRNA^{Gly}$ were identical in the absence and presence of the catalytic RNA (Figure 5). Likewise, the presence of M1 RNA did not affect the susceptibilities of anticodon loop nucleotides in $tRNA^{Gly}$ and DR4 (Figure 5).

DISCUSSION

Deletion of the Anticodon Arm. We have shown that the anticodon arm is of low significance for processing by HeLa extracts and the two bacterial RNase P enzymes (Table I). Even RNA ΔAC2, where the anticodon arm is replaced by a tetraloop sequence, was cleaved efficiently by the different RNase P activities. In addition, RNAs ΔAC1 and ΔAC2 showed the same inhibitory effect as $tRNA^{Gly}$ on pre-$tRNA^{Gly}$ cleavage (Figure 2), and the mature molecules bound to *E. coli* M1 RNA with very similar affinities as intact tRNA (Figures 3 and 4; Table II). At the beginning of our study, these results were not anticipated considering data reported by Pan et al. (1991). The authors used specific Pb^{2+}-induced hydrolysis of $tRNA^{Phe}$ in the D loop as a measure for perturbations of the tRNA structure by backbone breaks. In this assay, circularly permuted $tRNA^{Phe}$ molecules with single backbone breaks in the anticodon loop were cleaved in the D loop by lead ions at a 3–7-fold increased rate compared to the standard $tRNA^{Phe}$. On the basis of these data, an even stronger perturbation of the tRNA structure was expected for a variant with a deletion of the entire anticodon arm. However, Dichtl et al. (1993) reported normal lead-induced cleavage in the D loop of yeast $tRNA^{Phe}$ when the anticodon arm was replaced by certain tetranucleotides bridging the gap between the G26/A44 base pair. This suggests that ΔAC2 may have a tRNA-like core structure, which would explain its high cleavage efficiency (Table I).

No differences in the susceptibility of anticodon loop nucleotides of $tRNA^{Gly}$ and DR4 to Pb^{2+} hydrolysis were detected in the absence and presence of *E. coli* M1 RNA (Figure 5). This suggested that the conformation of anticodon loop nucleotides was unaffected by interaction with M1 RNA.

Role of the D Arm. T. thermophilus RNase P RNA and RNase P cleaved truncated $tRNA^{Gly}$ derivatives DR1–4 with a dramatically reduced activity (Table I). A comparably low activity was observed with a hairpin substrate, representing a truncated $tRNA^{Gly}$ reduced to acceptor stem and T arm (Schlegl et al., 1992). This suggests that substrates DR1–4 may provide no additional contact sites for complex formation beyond those already present in hairpin substrates mimicking the coaxially stacked acceptor stem and T arm.

Essentially identical results were obtained with HeLa extracts (Table I). All substrates carrying truncations of the D arm were processed poorly.

In contrast, RNase P from *E. coli* is highly active on substrates lacking the D arm (McClain et al., 1987; Table I) as well as on hairpin substrates (Forster & Altman, 1990; Schlegl et al., 1992), although these RNAs interact more weakly with *E. coli* M1 RNA (Figures 2–4) and RNase P (Schlegl et al., 1992). We have found in this study that low appK_d values of mature tRNA variants determined by gel retardation (Figure 4) correlated with strong inhibition effects of corresponding substrates or products in cleavage assays (Figure 2). The $tRNA^{Gly}$ and RNAs mΔAC1 and mΔAC2,

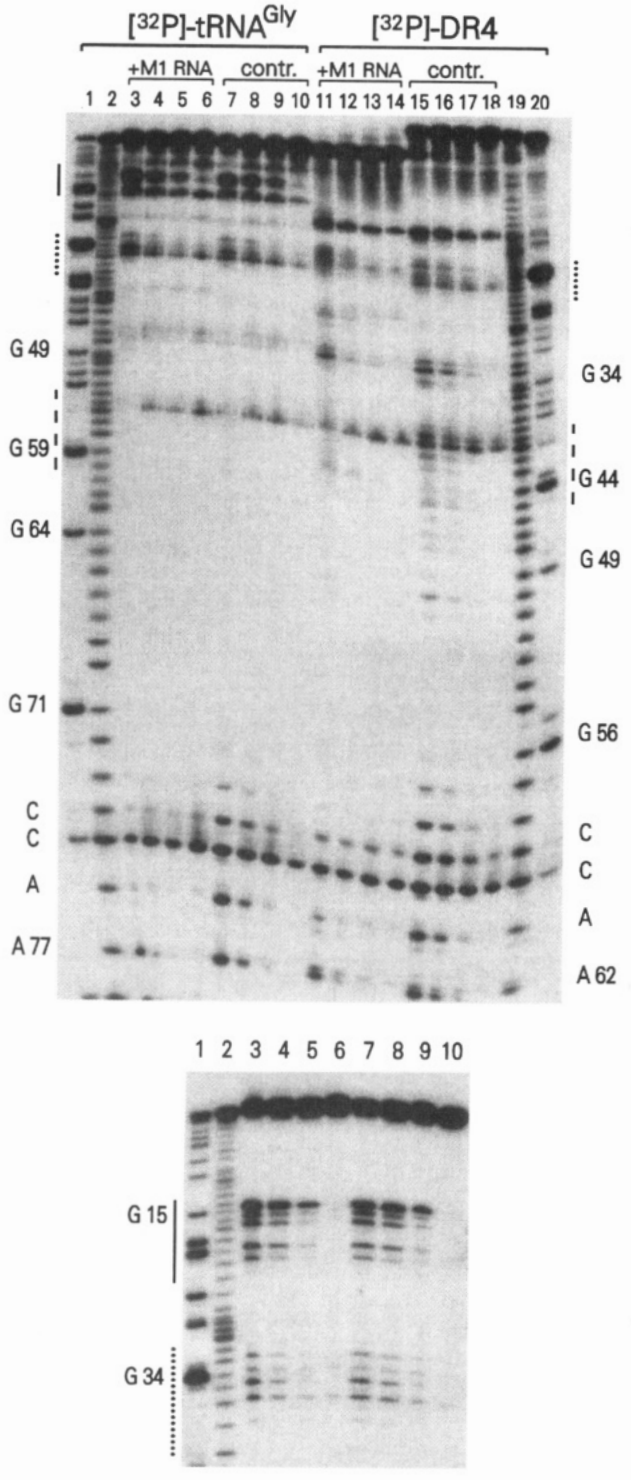

FIGURE 5: Pb^{2+}-induced cleavage of *T. thermophilus* $tRNA^{Gly}$ and DR4 in the presence or absence of *E. coli* M1 RNA. 25 ng of 3′-^{32}P-labeled DR4 or mature $tRNA^{Gly}$ was subjected to hydrolysis by Pb^{2+} ions for 15 min in the presence of 1.5 μg of unlabeled *E. coli* precursor 4.5S RNA (control, lanes 7–10 and 15–18) or 1.5 μg of unlabeled *E. coli* M1 RNA (lanes 3–6 and 11–14); assays were performed in 1 × TAMN without EDTA [100 mM $Mg(OAc)_2$, 100 mM NH_4OAc, and 50 mM Tris-HCl, pH 7.1]. Concentrations of $Pb(OAc)_2$ were as follows: lanes 6, 10, 14, and 18, no Pb^{2+} added; lanes 5, 9, 13, and 17, 20 mM Pb^{2+}; lanes 4, 8, 12, and 16, 50 mM Pb^{2+}; lanes 3, 7, 11, and 15, 100 mM Pb^{2+}; lane 2 and 19, limited alkaline hydrolysis, lanes 1 and 20, limited hydrolysis by RNase T1 (Ciesiolka et al., 1992a). In the case of DR4, the substrate is almost fully converted to mature DR4 in the presence of M1 RNA prior to addition of lead ions. The numbering system next to RNase T1 ladders corresponds to that in Figure 1; solid line, D-loop region; dotted line, anticodon loop region; dashed line, T-loop region. The upper panel shows a 25% polyacrylamide–8 M urea gel. In the lower panel, aliquots of the same samples analyzed in lanes 1–10 in the upper panel were run on a 10% polyacrylamide–8 M urea gel for better resolution of the D loop (solid line) and anticodon loop (dotted line) regions.

which had appK_d values of 0.07 and 0.1 μM (Figure 4, Table II), showed strong inhibitory effects in cleavage assays (Figure 2). In contrast, an appK_d value of 1.6 μM was determined for mDR4 (Figure 4), which is paralleled by a reduced inhibitory effect in the pre-$tRNA^{Gly}$ cleavage assay (Figure 2). Binding of mDR2 was even weaker (appK_d > 5 μM, data not shown), and no inhibition was observed in the cleavage assay (Figure 2B). The observation that the lower affinity of mDR4 to M1 RNA (appK_d = 1.6 μM) parallels a higher K_m of substrate DR4 in reactions of multiple turnover again supports the notion that the same structural elements which influence equilibrium binding of products to M1 RNA may also be relevant to the processing reaction.

The low-affinity binding to M1 RNA in combination with high cleavage efficiencies of substrates lacking the D arm suggests that the *E. coli* enzyme forms sufficiently strong contacts with the T arm, acceptor stem, and/or CCA terminus to still allow productive enzyme–substrate complex formation despite the loss of structural contributions provided by the D arm. If substrate interaction with intact tRNAs is already weak, as surmised for RNase P from *T. thermophilus* (Schlegl et al., 1992) and the HeLa enzyme preparation, any loss of contacts due to, for example, a different T-arm conformation would lead to a substantial decrease in activity. The question is raised whether *E. coli* RNase P is exceptional among enzymes of equal function.

The two mammalian mitochondrial tRNAs were cleaved with low efficiency by RNase P activities from *E. coli* (Table I). In our assay system, cleavage efficiencies of these RNAs were lower than those observed for hairpin substrates mimicking the coaxially stacked acceptor stem and T arm of *T. thermophilus* $tRNA^{Gly}$ (Schlegl et al., 1992). In light of the weaker enzyme–substrate interaction caused by D-arm deletions, the mt serine-tRNAs appear to lack structural features in the T arm and acceptor stem required for productive interaction. Low cleavage of mt serine tRNAs may also be attributable to a less rigid overall structure (Ueda et al., 1985). In earlier studies, enlarged T-loop structures per se (Figure 1) were not detrimental to cleavage by *E. coli* RNase P when implanted into a derivative of yeast $tRNA^{Phe}$ lacking the D arm (McClain et al., 1987).

Compared to the free $tRNA^{Gly}$, DR4 was more accessible to Pb^{2+}-induced hydrolysis in the T loop. This may indicate that T-loop conformations differ in tRNA and variants lacking the D arm. Under conditions of equilibrium binding to *E. coli* M1 RNA, we observe reduced lead-induced hydrolysis of mDR4 at the CU*CCA*A 3′-terminus and in the T arm (Figure 5). The latter region has been inferred as a general RNase P contact region from modification interference studies (Kahle et al., 1990; Thurlow et al., 1991).

Our kinetic and equilibrium binding data suggest that the structure of the elbow of L-shaped tRNAs is an essential recognition determinant in the reaction catalyzed by RNase P enzymes. It has been shown recently for two different tRNAs by modification interference that T-loop nt 54 and 55 at the elbow are potential contact sites (Gaur & Krupp, 1993).

In the presence or absence of *E. coli* RNA, patterns of Pb^{2+}-induced hydrolysis were identical in the D loop of $tRNA^{Gly}$ (Figure 5). This may indicate that the D arm is not

in direct contact with the enzyme. In this case, the structural contribution of the D arm would be to maintain the authentic geometry at the elbow, rendering the T loop in the optimal conformation for recognition by RNase P enzymes. This would be in accordance with modification interference studies, which gave indications for specific contacts between RNase P and substrates in the acceptor stem and the T arm, but not in the D loop (Kahle et al., 1990; Thurlow et al., 1991; Gaur & Krupp, 1993). However, on the basis of the lead hydrolysis assay, we cannot exclude direct contacts of the D arm with M1 RNA, since the small lead probe may leave more remote contacts of tRNA and RNase P RNA undetected as long as coordination geometries at hydrolysis sites remain unchanged. In addition, the Pb^{2+} aquo cation attacks the phosphate–sugar backbone, and may not sense changes in base reactivity.

In summary, it becomes evident that the anticodon arm is likely to be of marginal importance for interaction with RNase P enzymes in general. This is consistent with chemical modification interference studies which showed low interference of modifications in the anticodon arm with RNase P cleavage (Kahle et al., 1990; Thurlow et al., 1991). In contrast, the D arm contributes to recognition by RNase P enzymes. The deletion of this structural element, however, had different effects on processing by the RNase P activities analyzed here.

ACKNOWLEDGMENT

We thank Werner Schröder for the synthesis of DNA oligonucleotides and Silke Volkmann, Gerd Vorbrüggen, and Karin Mölling for the HeLa extracts. Plasmid pJA2 was a gift from Cecilia Guerrier-Takada and Sidney Altman, and plasmid T7-4.5S was kindly provided by Richard A Lempicki and Maurille J. Fournier. We thank Rolf Bald and Jens Peter Fürste for chemical synthesis of the 14-nt RNA (5′ flank).

REFERENCES

Behlen, L. S., Sampson, J. R., DiRenzo, A. B., & Uhlenbeck, O. C. (1990) *Biochemistry 29*, 2515–2523.
Brown, J. W., & Pace, N. R. (1992) *Nucleic Acids Res. 20*, 1451–1456.
Brown, R. S., Dewan, J. C., & Klug, A. (1985) *Biochemistry 24*, 4785–4801.
Ciesiolka, J., Lorenz, S., & Erdmann, V. A. (1992a) *Eur. J. Biochem. 204*, 575–581.
Ciesiolka, J., Lorenz, S., & Erdmann, V. A. (1992b) *Eur. J. Biochem. 204*, 583–589.
Cronenberger, J. H., & Erdmann, V. A. (1975) *J. Mol. Biol. 95*, 125–137.
De Bruijn, M. H. L., & Klug, A. (1983) *EMBO J. 2*, 1309–1321.
De Bruijn, M. H. L., & Klug, A. (1984) *Alfred Benzon Symp. 19*, 259–278.
Dichtl, B., Pan, T., DiRenzo, A. B., & Uhlenbeck, O. C. (1993) *Nucleic Acids Res. 21*, 531–535.
Dignam, J. D., Lebovitz, R. M., & Roeder, R. G. (1983) *Nucleic Acids Res. 11*, 1475–1489.
England, T. E., & Uhlenbeck, O. C. (1978) *Nature 275*, 560–561.
Forster, A. C., & Altman, S. (1990) *Science 249*, 783–786.
Garey, J. R., & Wolstenholme, D. R. (1989) *J. Mol. Evol. 28*, 374–387.
Gaur, R. K., & Krupp, G. (1993) *Nucleic Acids Res. 21*, 21–26.
Guerrier-Takada, C., & Altman, S. (1993) *Biochemistry 32*, 7152–7161.
Guerrier-Takada, C., Gardiner, K., Marsh, T., Pace, N., & Altman, S. (1983) *Cell 35*, 849–857.
Hardt, W.-D., Schlegl, J., Erdmann, V. A., & Hartmann, R. K. (1993) *Nucleic Acids Res. 21*, 3521–3527.
Hartmann, R. K., & Erdmann, V. A. (1991) *Nucleic Acids Res. 19*, 5957–5964.
Hartmann, R. K., Toschka, H. Y., & Erdmann, V. A. (1991) *J. Bacteriol. 173*, 2681–2690.
Kahle, D., Wehmeyer, U., & Krupp, G. (1990) *EMBO J. 9*, 1929–1937.
Krzyzosiak, W. J., Marciniec, T., Wiewiorowski, M., Romby, P., Ebel, J. P., & Giegé, R. (1988) *Biochemistry 27*, 5771–5777.
McClain, W. H., Guerrier-Takada, C., & Altman, S. (1987) *Science 238*, 527–530.
Milligan, J., F., & Uhlenbeck, O. C. (1989) *Methods Enzymol. 180*, 51–62.
Okimoto, R., & Wolstenholme, D. R. (1990) *EMBO J. 9*, 3405–3411.
Pan, T., Gutell, R. R., & Uhlenbeck, O. C. (1991) *Science 254*, 1361–1364.
Pyle, A. M., McSwiggen, J. A., & Cech, T. R. (1990) *Proc. Natl. Acad. Sci. U.S.A. 87*, 8187–8191.
Quigley, G. J., & Rich, A. (1976) *Science 194*, 796–806.
Schlegl, J., Fürste, J. P., Bald, R., Erdmann, V. A., & Hartmann, R. K. (1992) *Nucleic Acids Res. 20*, 5963–5970.
Smith, D., Burgin, A., Haas, E. S., & Pace, N. R. (1992) *J. Biol. Chem. 267*, 2429–2436.
Sprinzl, M., Hartmann, T., Weber, J., Blank, J., & Zeidler, R. (1989) *Nucleic Acids Res. 17*, r1-r172.
Tallsjö, A., & Kirsebom, L. A. (1993) *Nucleic Acids Res. 21*, 51–57.
Thurlow, D. L., Shilowski, D., & Marsh, T. L. (1991) *Nucleic Acids Res. 19*, 885–891.
Ueda, T., Ohta, T. & Watanabe, K. (1985) *J. Biochem. 98*, 1275–1284.
Vioque, A., Arnez, J., & Altman, S. (1988) *J. Mol. Biol. 202*, 835–848.